JACS
JOURNAL OF THE AMERICAN CHEMICAL SOCIETY
Communication
Cite This: J. Am. Chem. Soc. 2019, 141, 5083−5086
pubs.acs.org/JACS

J. Am. Chem. Soc. 2019, 141, 5083−5086

Site-Selective Growth of Crystalline Ceria with Oxygen Vacancies on Gold Nanocrystals for Near-Infrared Nitrogen Photofixation

Henglei Jia,[†] Aoxuan Du,[†] Han Zhang,[‡] Jianhua Yang,[‡] Ruibin Jiang,[*,§] Jianfang Wang,[*,‡] and Chun-yang Zhang[*,†]

[†]College of Chemistry, Chemical Engineering and Materials Science, Collaborative Innovation Center of Functionalized Probes for Chemical Imaging in Universities of Shandong, Key Laboratory of Molecular and Nano Probes, Ministry of Education, Shandong Provincial Key Laboratory of Clean Production of Fine Chemicals, Shandong Normal University, Jinan 250014, China.
[‡]Department of Physics, The Chinese University of Hong Kong, Shatin, Hong Kong SAR, China.
[§]Shaanxi Engineering Lab for Advanced Energy Technology, School of Materials Science and Engineering, Shaanxi Normal University, Xi'an 710119, China.

Amrita Chakraborty

11-05-2019

Relevance to the group

1. Anisotropic gold nanoparticle
2. Synthesis of heterostructure
3. Application

Background

Hot electrons: Electrons not in thermal equilibrium with the atoms in a material.
When a material is illuminated with highly energetic photons (for example, ultraviolet radiation), hot electrons are generated and emitted from the material via the photoelectric effect.

Schottky Barrier: When a metal or superconductor makes intimate contact with a semiconductor,

1. the Fermi levels in the two materials must be equal at thermal equilibrium.
2. the vacuum level must also be continuous.

These two requirements result in band bending at the interface creating a potential barrier known as the Schottky barrier. This gives a unique energy band diagram for the contact for each such pair.

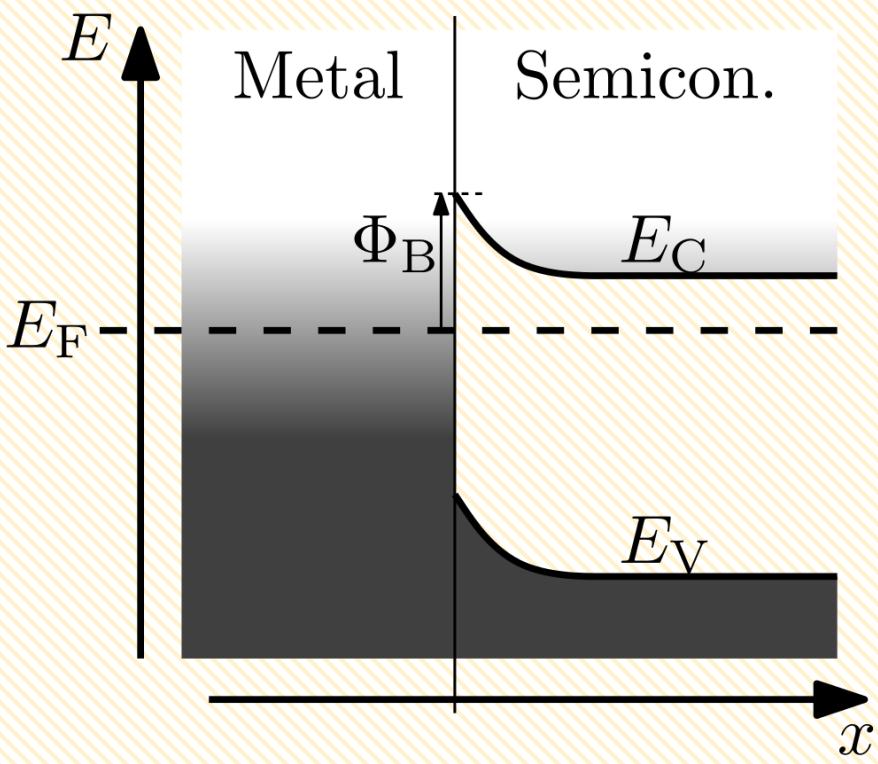

Band diagram for n-type semiconductor Schottky barrier at zero bias (equilibrium): Schottky barrier height, Φ_B is the difference between the interfacial conduction band edge E_C and Fermi level E_F.
For a p-type Schottky barrier, Φ_B is the difference between E_F and the valence band edge E_V.

Introduction

- Solar energy can trigger various challenging reactions to take place under mild and environmentally friendly conditions.
- Challenge : poor visible and NIR photocatalytic activity of traditional oxide semiconductor photocatalysts.
- Solution : integration of oxide semiconductors with plasmonic metal nanocrystals, e.g., Au nanocrystals, which can efficiently extend the photocatalytic activity of semiconductors to the visible and NIR regions through the hot-electron injection mechanism.
- Once hot electrons are injected into the semiconductor, holes left on Au nanocrystals should be consumed simultaneously, otherwise the accumulation of holes will prevent the further injection lowering the photocatalytic activity.
- The ideal plasmonic photocatalysts should have spatially separated structures that allow holes and electrons to participate in the reaction simultaneously.
- Selective coating of crystalline oxide semiconductors on the ends of Au NRs has not been reported so far, because the decomposition of oxide precursors generally requires >400 °C, which makes the reaction dynamics difficult to control, also Au NRs deform and agglomerate.

In this paper

- CeO_2 as an n-type semiconductor is a good candidate for plasmonic photocatalysis, because it can form an appropriate Schottky barrier with Au nanocrystals to facilitate the hot-electron injection.
- The ceria-based materials possess excellent catalytic capability due to the extensive presence of oxygen vacancies on their surfaces.
- Benefiting from the tunable longitudinal plasmon wavelength, the large extinction cross sections, and the preferential hot-electron generation on the ends, Au NRs are of particular interest as the core.
- They report a facile wet-chemistry route for the selective growth of crystalline ceria at the ends of gold nanorods (Au NRs) in the presence of a small amount of bifunctional K_2PtCl_4.
- The obtained heteronanostructures are Au NRs capped with crystalline ceria at the ends (i.e., Au/end-CeO2). Such a spatial distribution makes hot electrons participate in the reduction reaction at the ends and hot holes be consumed at the exposed side surface, greatly enhancing the utilization efficiency of photocarriers.

Synthesis of GNR/end-CeO2 nanostructure

- 10 mL as-grown GNR was cleaned and redispersed into CTAB solution (0.1 mM, 5 mL).
- The K_2PtCl_4 solution (0.1 mM, 200 uL) was subsequently added into the Au NR solution under gentle shaking. The resultant solution was kept at room temperature for 2 min to allow for the adsorption of $PtCl_4^{2-}$ on the Au NRs.
- Because of the crystal structure and the curvature difference, the molecular chains of CTAB at the ends are less dense in space than those on the side surface. Due to smaller steric hindrance $PtCl_4^{2-}$ preferentially adsorb at two ends of Au NR.
- A freshly prepared $Ce(AC)_3$ solution (10 mM, 500 uL) and DI water (4.3 mL) were sequentially added into the Au NR solution under gentle shaking.
- The resultant solution was placed in an oven set at 100 °C for 1 h. The ceria precursor, $Ce(AC)_3$ can be rapidly hydrolyzed into $Ce(OH)_3$ at > 60 °C and then oxidized by the pre-adsorbed $PtCl_4^{2-}$ according to the autoredox reaction . This serves as the nuclei for the further growth of CeO_2. This results in a site-selective nucleation and growth of CeO_2, generating Au/end-CeO_2 heteronanostructure.
- The product was washed by centrifugation and redispersed in DI water (10 mL) for further use.

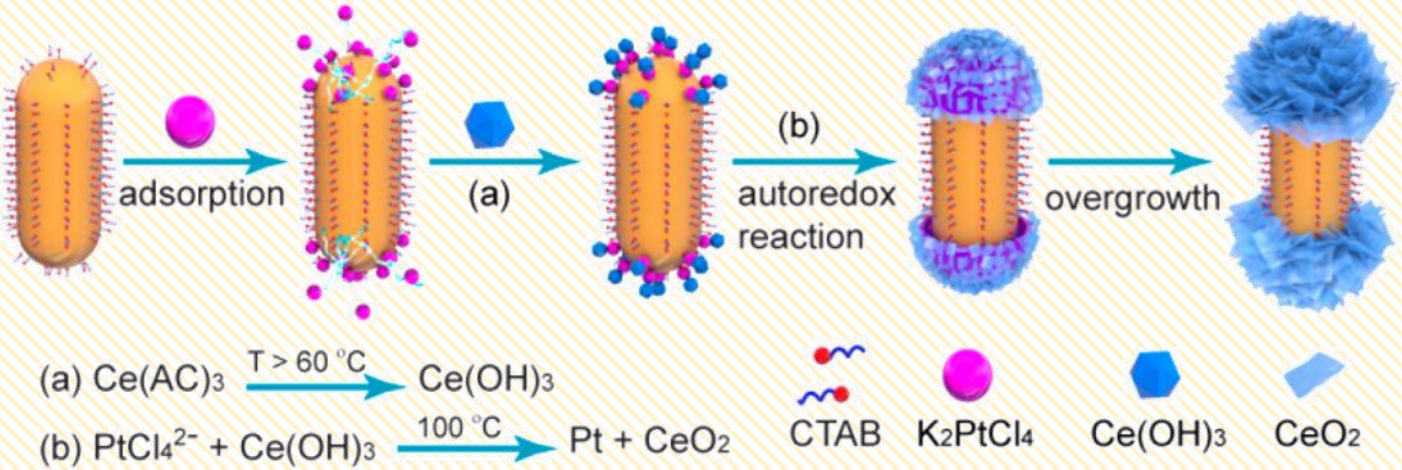

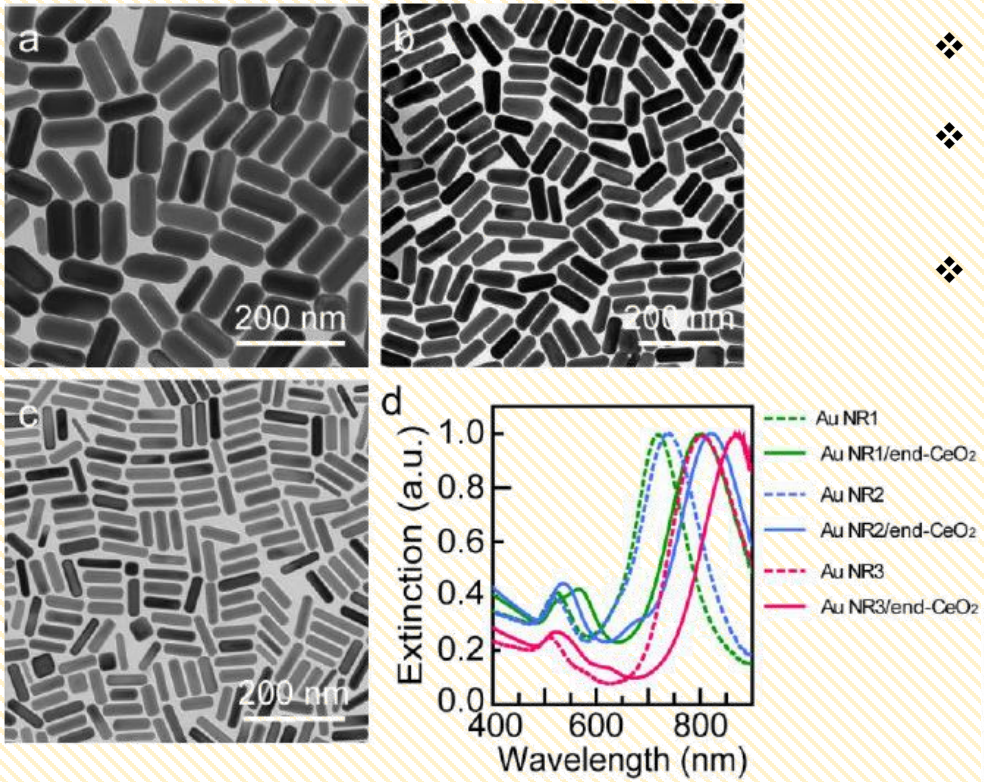

Figure S1. (a−c) TEM images of three starting Au NR samples. (d) Extinction spectra of three Au NR samples before (dashed lines) and after (solid lines) the selective coating of CeO_2. The average diameters of the Au NRs are 40.6 □ 3.1 nm, 31.6 □ 2.3 nm, and 18.3 □ 1.4 nm,

- Three Au NR samples with different aspect ratios were used for the ceria growth .
- The thicknesses of the CeO_2 layer in three samples are 12.9 ± 1.8 nm, 15.0 ± 1.8 nm and 12.5 ± 1.6 nm, respectively.
- Owing to the larger refractive index of CeO_2 relative to water, the longitudinal plasmon resonance peaks of the Au NRs exhibit a redshift after the end-coating of CeO_2.

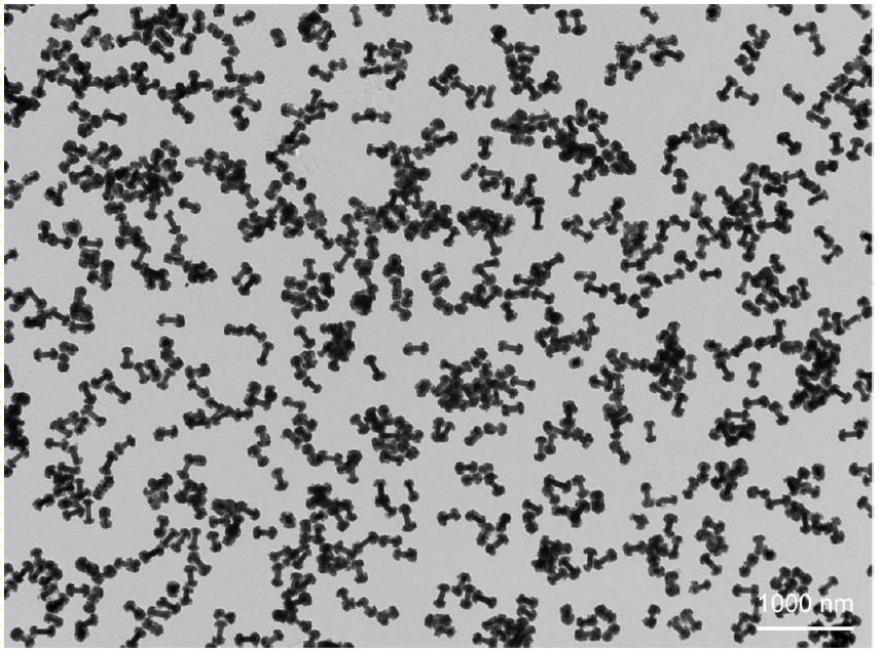

Figure S2. Representative TEM image of the Au NR/end-CeO_2 nanostructures at a low magnification. Yield = 96%

Structure and chemical composition of the composite

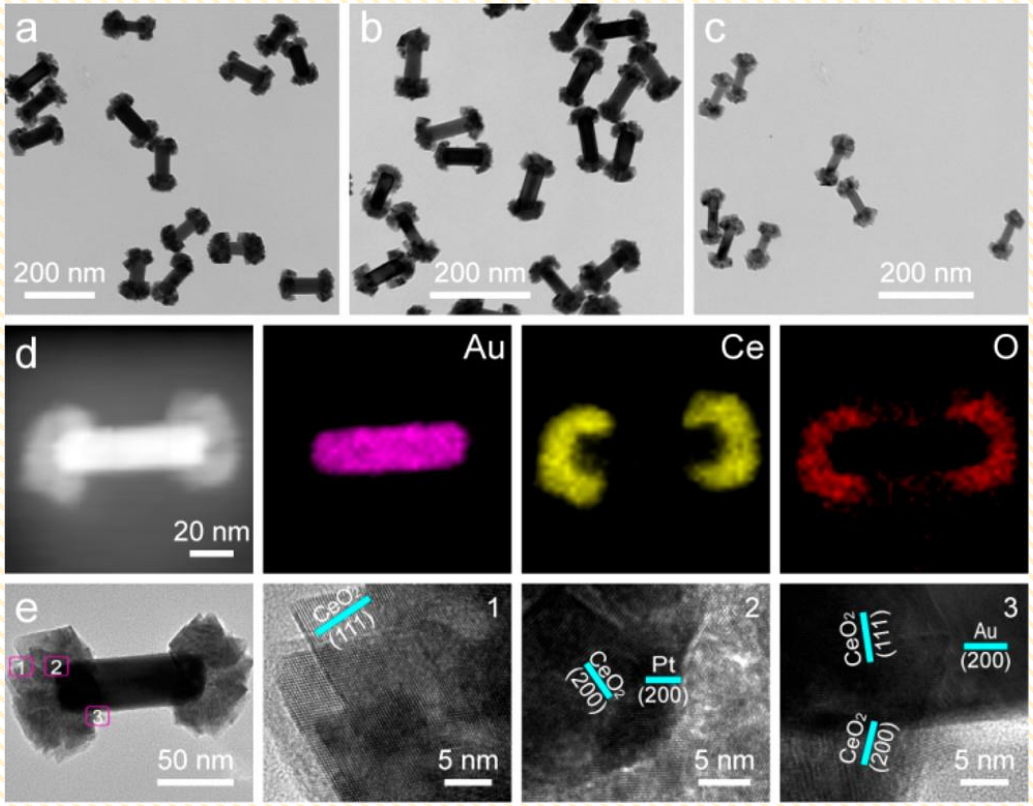

Figure 2. (a–c) TEM images of the Au/end-CeO2 nanostructures produced from three different sized Au NRs. (d) HAADF-STEM image and the corresponding elemental maps. (e) HRTEM images of a single Au/end-CeO2 nanostructure.

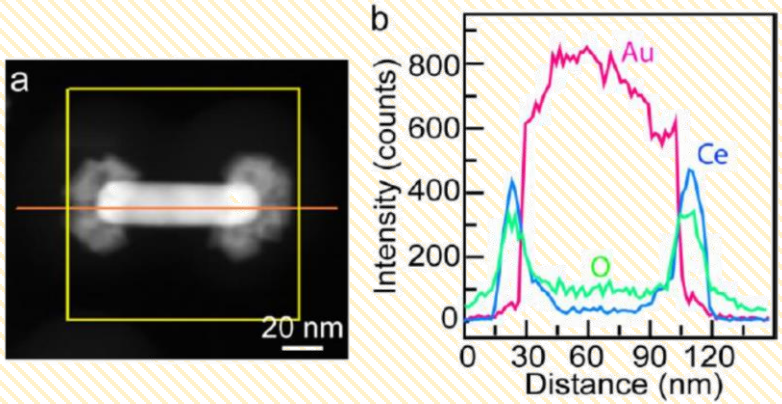

Figure S3. Elemental profiles of a single Au/end-CeO2 nanostructure. (a) HAADF-STEM image. (b) Elemental profiles of Au, Ce and O acquired along the orange line indicated in (a).

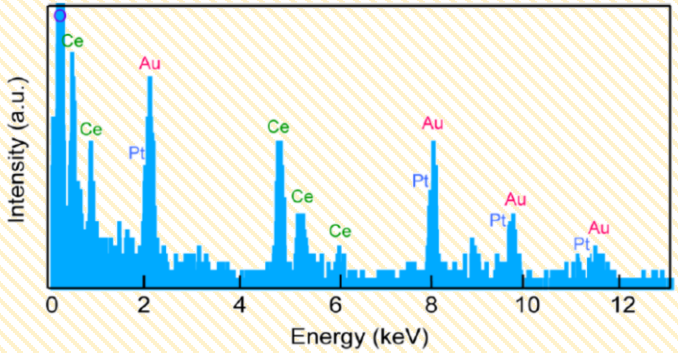

Figure S4. EDX spectrum of a representative Au/end-CeO2 nanostructure.

Element valence states and OVs

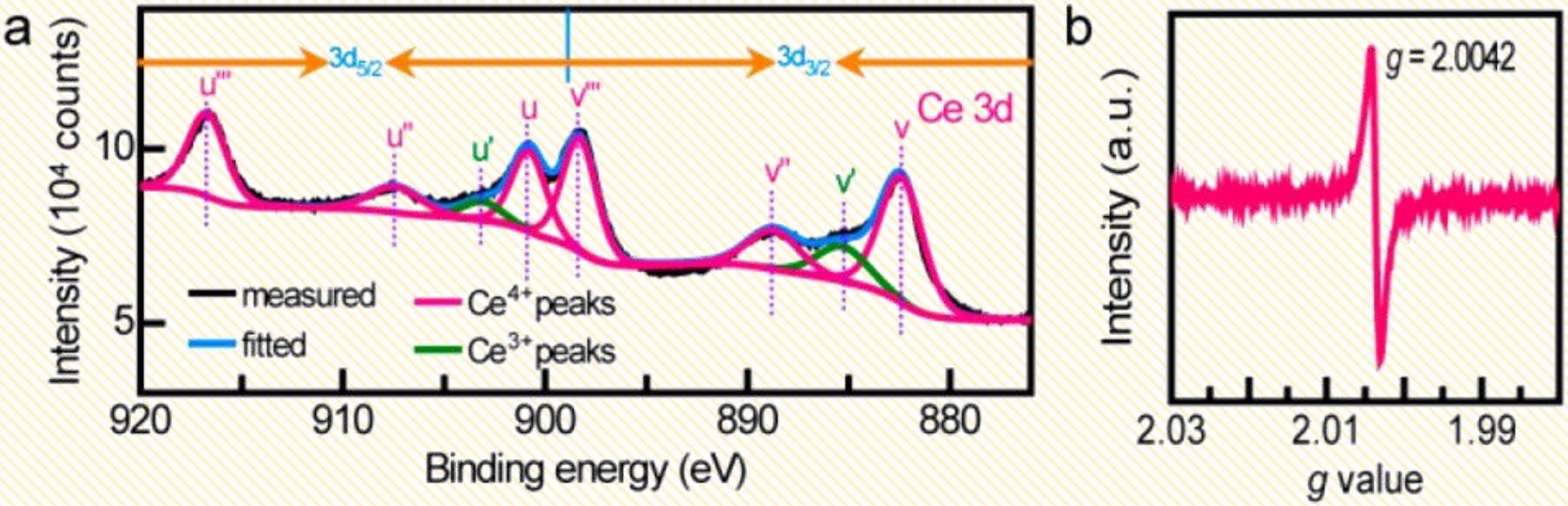

Figure 3. High-resolution Ce 3d XPS spectrum (a) and EPR spectrum (b) of the Au/end-CeO_2 nanostructures.

- The presence of Ce^{3+} implies the defect structure CeO_{2-x} in CeO_2 due to oxygen vacancies. This transformation of Ce^{4+} to Ce^{3+} driven by oxygen vacancies may be the key to understanding the catalytic properties of ceria.
- Ratio of Ce(IV) to Ce(III) = 85:15 (integrating the peak areas). This result suggests that the dominant form of Ce is Ce(IV).
- EPR peak with g = 2.0042 indicates the formation of OVs caused by the Ce(III) state.

Control experiments

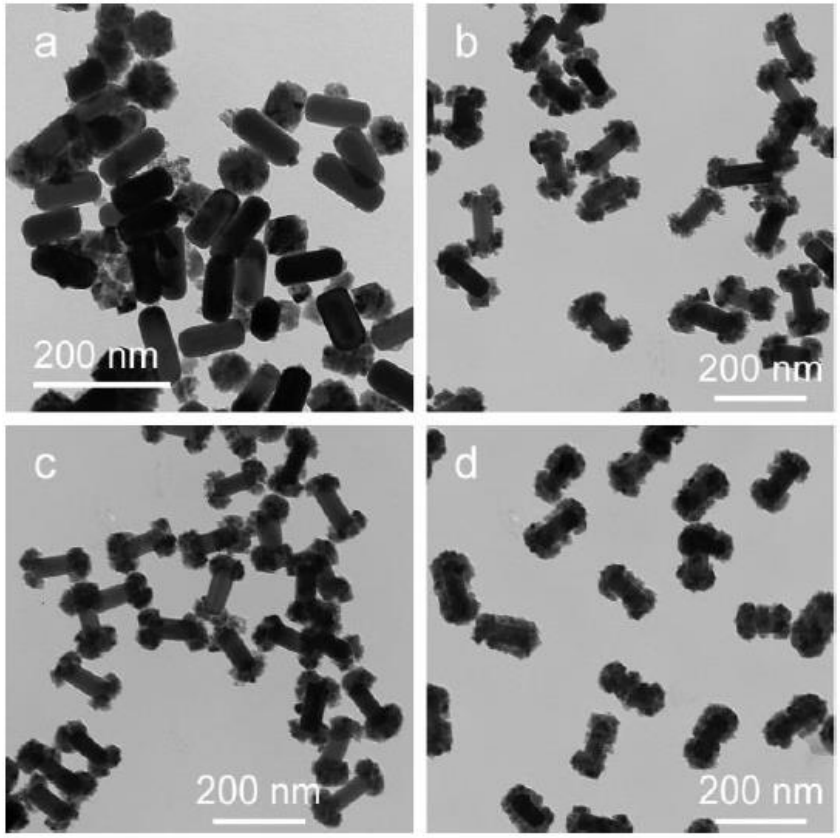

Figure S7. Effect of the amount of K_2PtCl_4 :
0 µL (a), 50 µL (b), 200 µL (c), and 2000 µL (d)

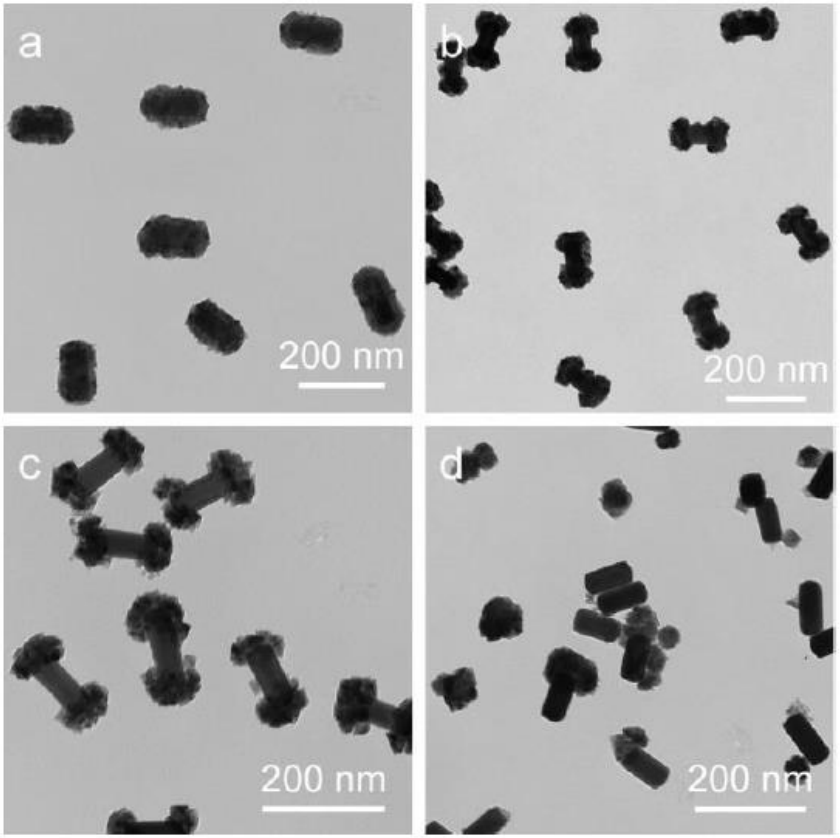

Figure S8. Effect of the CTAB concentration :
5 µM (a), 20 µM (b), 50 µM (c), and 200 µM (d),.

Nitrogen fixation experiment

- N_2 fixation is industrially accomplished at high temperatures and high pressures because a large activation barrier (~941 kJ/mol) should be overcome.
- N_2 molecules can be chemisorbed and activated by Ovs and reduced to NH_3 by the injected plasmonic hot electrons.
- AuNR, Au/end-CeO_2 and a fully coated Au@CeO_2 core@shell nanostructure with longitudinal plasmon wavelengths finely adjusted as closely as possible to the laser wavelength, were compared.
- The spatially separated structure and the presence of OVs make the Au/end-CeO_2 nanostructures a preferable candidate for plasmon-induced NIR N_2 photofixation.

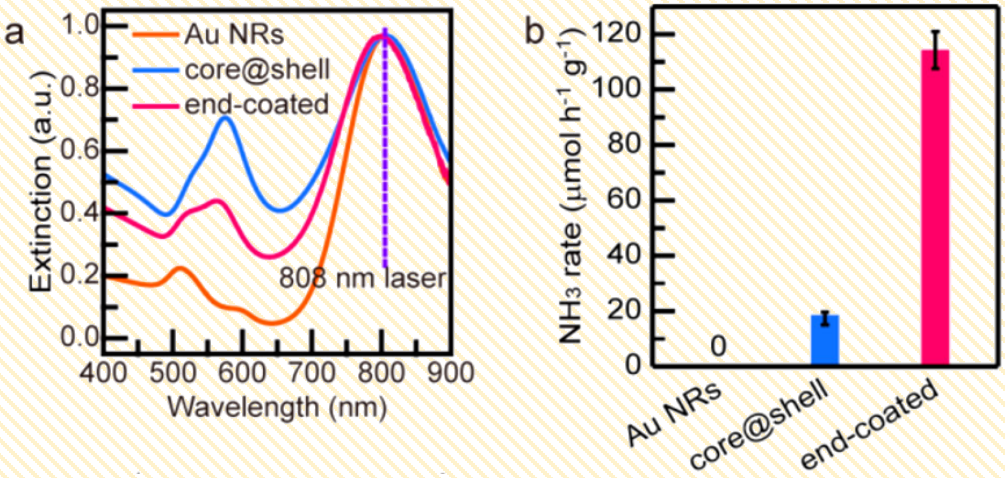

Figure 4. Plasmonic N2 photofixation under NIR illumination. (a) Extinction spectra of three photocatalyst nanostructures. (b) N2 photofixation rates of three photocatalysts.

9,10-Anthracenediyl-bis(methylene)dimalonic acid

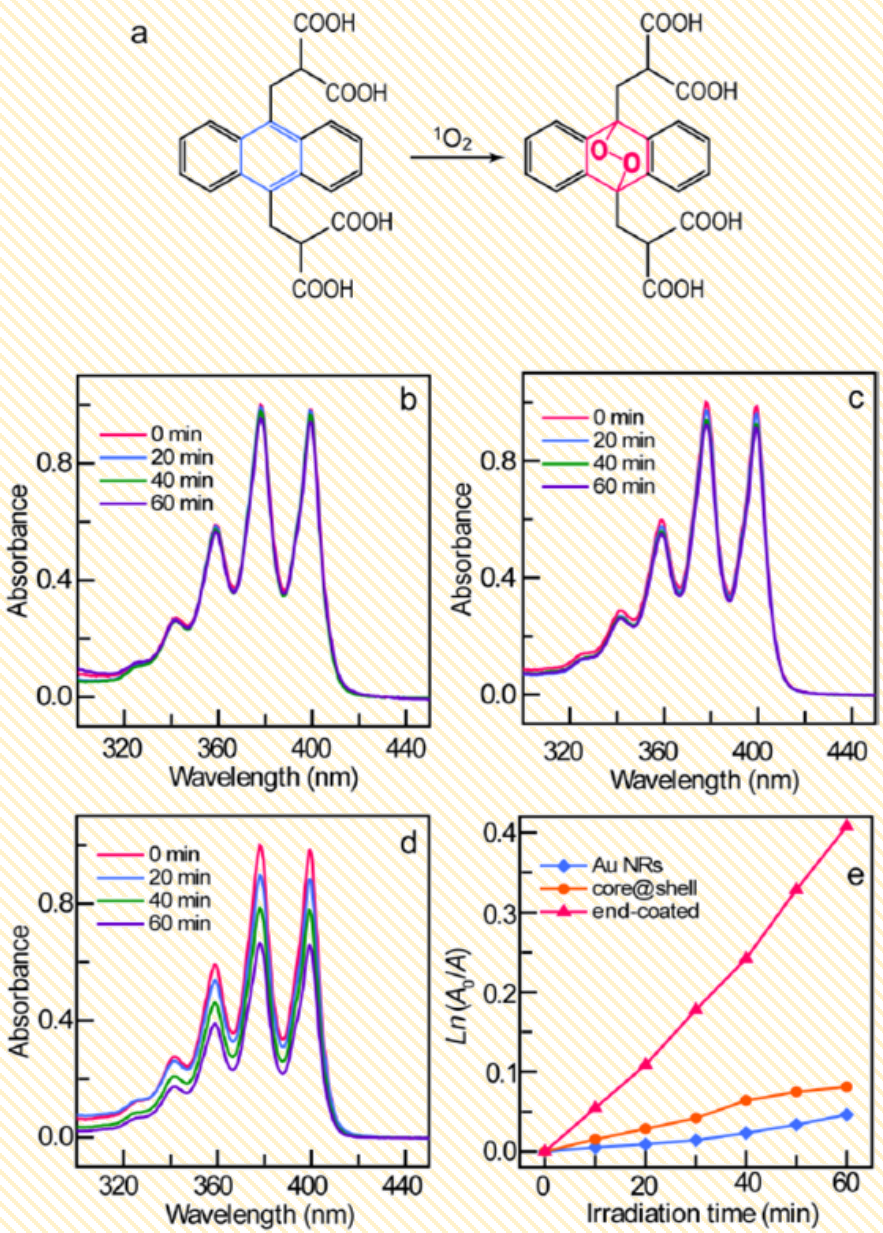

- Rate constant of Au/end-CeO_2 = 0.68 × 10^{-2} min^{-1},
- 8.9 fold of AuNR
- 5.0-fold of the core@shell nanostructures
- The spatially separated structure facilitates the electron−hole separation.

Figure S10. Singlet oxygen generation with different photocatalysts. (a) Schematic of the reaction between ABDA and $^1O_2$. (b−d) Normalized time-dependent absorption spectra of ABDA obtained with the Au NR nanostructure (b), the core@shell nanostructure (c), and the Au/end-CeO2 nanostructure (d) as the photocatalysts, respectively. (e) Variance of 1O2 generation rates as a function of the time with different photocatlysts under NIR illumination. The generation rate constants are calculated by assuming first-order reaction kinetics.

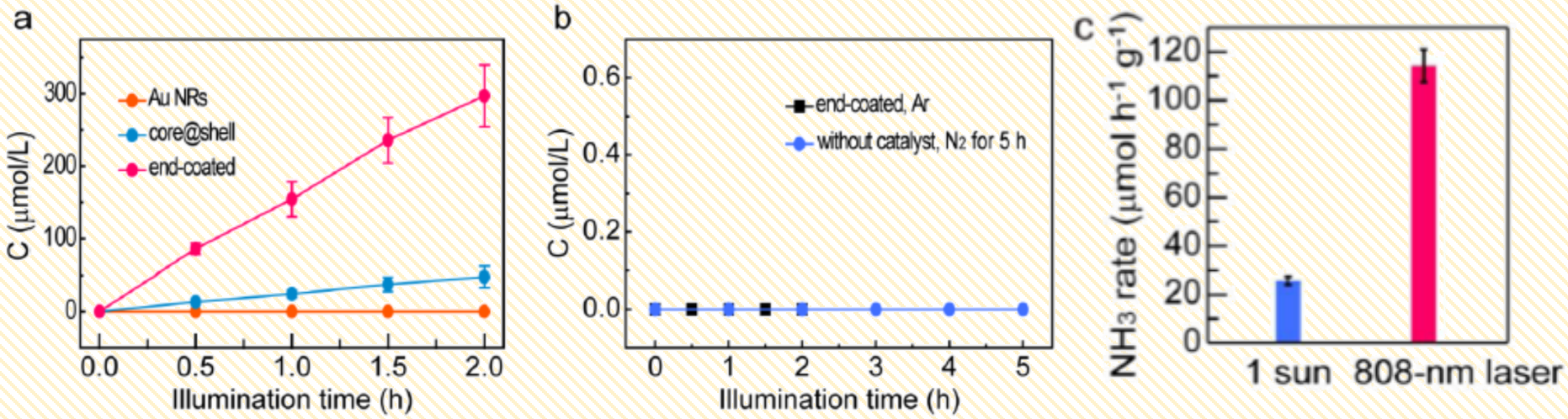

Figure S12. (a) Time-dependent ammonia generation for three types of catalysts. (b) Control experiments in Ar environment and without catalyst, respectively c) Comparison of the N_2 photofixation rates under 1 sun illumination and the 808-nm laser illumination.

- The concentration of NH_3 increases linearly with the reaction time for the core@shell and the end coated samples as the catalysts, while AuNR shows no NIR photocatalytic activity.
- No NH_3 was detected by substituting N_2 with Ar , suggesting that NH_3 was generated by the reduction of N_2 .
- NH_3 did not come from the contamination and the impurity, because no NH_3 was detected after bubbling of N_2 under laser illumination for 5 h without the catalyst.
- The N_2 fixation rate of the Au/end-CeO_2 nanostructure is 114.3 μmol·h−1·g−1 under the 808 nm laser illumination, which is 6.2-fold compared with that of the core@shell nanostructure.
- Proof-of-concept: N_2 fixation rate of Au/end-CeO_2 under 1 sun illumination = 25.6 μmol·h−1·g−1

Possible mechanism : plasmon-induced NIR N2 photofixation

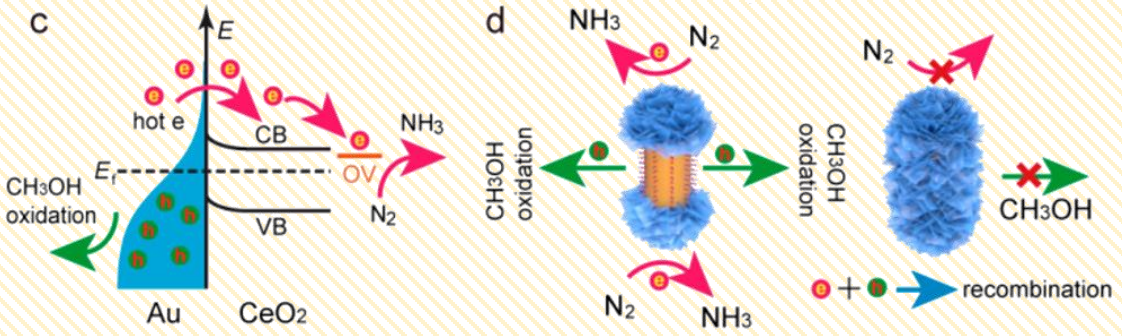

Figure 4 (c) Mechanism of N2 photofixation for the Au/end-CeO2 nanostructures. Ef, Fermi level; CB, conduction band; VB, valence band; OV, oxygen vacancy states. (d) Comparison of the hot carrier separation behaviors of the Au/end-CeO2 nanostructure with that of the core@shell nanostructure.

- The inherent OV states (i.e., Ce^{3+}) on the surface of CeO_2 act as the catalytic active sites that chemisorb and activate N_2 molecules.
- Under the plasmon excitation, Au NRs absorb NIR light to generate hot electrons and hot holes. This hot electrons are injected into the CB of CeO_2 across the Schottky barrier, followed by the transport to the OV states where the adsorbed and activated N_2 is reduced into NH_3.
- Meanwhile, the hot holes are consumed by the hole scavengers at the side of the Au NRs to complete the photocatalytic cycle.
- The spatial separation design of the Au/end- CeO_2 nanostructures offers reaction sites for both reduction and oxidation, with the reduction of N_2 occurring on the surface of CeO_2 and the consumption of hot holes on the side surface of the Au NRs.
- In contrast, in the core@shell nanostructures, the Au NRs are buried inside, making hot holes be hardly accessed by CH_3OH that results in the electron−hole recombination. A small activity obtained on the core@shell nanostructures may result from the presence of tiny gaps among the CeO_2 nanosheets.

Summary

- A new type of spatially separated nanostructure is designed and synthesized by selectively coating crystalline ceria on the Au NRs using a wet-chemistry strategy at a moderate temperature.
- This was achieved with the assistance of bifunctional K_2PtCl_4 that selectively adsorb on two ends of Au NRs and trigger the autoredox reaction of the ceria precursor.
- The presence of OVs in combination with the spatial separation structure makes the Au/end-CeO_2 an excellent candidate for plasmon-induced NIR N_2 photofixation.
- Further improvement of the NIR photocatalytic activity may be accomplished by either extending the light absorption with different Au/end-CeO_2 mixtures or engineering with the cocatalysts.
- They postulate that the proposed selective growth strategy will motivate the rational design of various spatial-separated plasmonic nanostructures for novel photocatalytic applications.


thank
you!